Characterization of the gas effluent in the treatment of nitrogen containing pollutants in water by Fenton Process

J. Carbajo*, A. Quintanilla, J.A. Casas

Chemical Engineering Department, Universidad Autonoma de Madrid, Ctra. Colmenar km. 15, 28049 Madrid, Spain.

*Corresponding author: jaime.carbajo@uam.es

Abstract

This work evidences for the first time the production of CO and NO_x during the removal of nitrogen containing pollutants in water by Fenton Process, the most popular method for Advanced Oxidation Processes. Four representative nitrogen containing pollutants were selected, *viz.* aniline, 4-nitrophenol, pyridine and monoethanolamine. The gas effluent accumulated after 3 h of reaction at 90 °C and 3 bar was analysed. In all cases, the carbon and nitrogen mass balance was assessed. Also, an on-line off-gas analysis system was set up to monitor the off-gas variation of CO and CO_2 from the beginning of the reaction.

CO_2 was the major component of the gas effluent. It was progressively produced upon oxidation. In contrast, CO was detected in fairly lower amounts and it was immediately produced after H_2O_2 injection, due to the rupture and opening of the aromatic ring. The CO formation was more favorable upon degradation of aromatic than aliphatic compounds, or when the nitrogen was in the aromatic ring, as in the case of pyridine. The nitrogen functional groups were majorly transformed into NH_4^+ and NO_3^-, while NO_x was detected in low amounts (<1 mg/m^3) and favoured in presence of $–NO_2$ group.

These results highlight the importance of monitoring the gas phase generated in the treatment of high-loaded wastewater by AOPs in order to guarantee the environmental sustainability of the processes.

Keywords: N-containing organic compounds; gas monitoring; CO and NO_x formation; Fenton process; advanced oxidation process.

1. Introduction

The most stringent emission limits for toxic and priority pollutants require more efficient technologies to meet the current water quality standards [1]. Advanced Oxidation Processes (AOPs) are considered effective and environmentally sustainable technologies to remove persistent organic pollutants from water [2, 3] or to convert them into biodegradable compounds [4, 5, 6, 7]. These technologies involve the *in-situ* production of hydroxyl radicals ($HO^{\bullet}$) at sufficient concentration to effectively react with the pollutants in water, oxidizing them. A gas effluent is produced due to the formation of gaseous compounds from the oxidation of organic pollutants [8].

A great number of processes are classified under the definition of AOPs. Most of them use a combination of strong oxidizing agents (*e.g.* H_2O_2, O_3) with catalysts (*e.g.* transition metal ions, metallic nanoparticles or carbon based catalysts) and irradiation (*e.g.* ultraviolet, visible, microwave), sonication or electrolysis [9-15]. The wide variety of industrial discharges make necessary the selection of the better-performing process adapted to each situation, processes that must integrate wastewater and gas treatment to assure the effectiveness and sustainability expected by obtaining environmentally compatible effluents [16].

Hazardous pollutants can be successfully removed from water if the treatment conditions are adequately controlled. The composition of the resulting gas effluent depends on the

nature of the pollutant itself [16, 17] and also on the treatment conditions as far as they directly affect the intermediate distribution [16]. The recent study of Carbajo et al. [16] devoted to the characterization of the gas effluents in Fenton Oxidation Process revealed for the first time the formation of significant amounts of CO, along with CO_2, as carbon gaseous compounds upon the treatment of high-loaded phenolic wastewater. It was demonstrated that CO was mainly formed during the oxidative cleavage of aromatic rings. In case of the treatment of nitrogen-containing pollutants by AOPs, different N-gaseous species have been detected in recent studies [17, 18]. Thus, harmless molecular N_2 was the only nitrogen species in the off-gas effluent during the CWAO of ammonia [18] while traces of NO and NO_2 (three order of magnitude lower than the initial nitrogen in solution) were detected upon the electrochemical oxidation of 670 mg/L of 4-nitrobenzoic acid and several substituted aminobenzoic acids [17]. In none of these works, the N balance was analysed, neither CO nor CO_2 were measured in the gas effluent.

Considering the industrial implementation of the Fenton Process for the treatment of different types of non-biodegradable industrial wastewater such as pharmaceutical, cosmetic, refinery or petrochemical wastewater [6,19], which can contain high concentrations of nitrogen pollutants, it seems pertinent the assessment of the gas effluent in the course of the Fenton process to specially evaluate the formation and emission of noxious gaseous species such as CO and NO_x.

Herein, four representative nitrogen containing pollutants, *viz*. aniline (AN), 4-nitrophenol (4NPH), pyridine (PYR) and monoethanolamine (MEA), have been selected (their corresponding chemical structures are shown in Figure S1 of the Supplementary Material). A precise determination of CO, CO_2 and NO_x amounts in the gas phase and the total carbon and nitrogen content in the liquid phase has allowed the accurate analysis of the carbon and nitrogen mass balance. An on-line off-gas analysis system was set up to

monitor the off-gas variation of CO and CO_2, the most representative species in the gas effluent, upon oxidation reaction. This study provides a good overview of the effectiveness and sustainability of the AOPs processes for the treatment of nitrogen containing pollutants and, in particular, a better understanding of the potential gaseous noxious emissions in Fenton processes.

2. Experimental

2.1. Chemicals

Hydrogen peroxide solution (30% w/v) and $FeCl_2 \cdot 4H_2O$ (>98.0 %) were purchased from Sigma-Aldrich. Standard solutions of phenol (Sigma-Aldrich), aniline (Panreac), 4-nitrophenol (Panreac), monoethanolamine (Sigma-Aldrich), ammonium chloride (Sigma-Aldrich), $NaNO_3$ (Panreac) and $NaNO_2$ (Panreac) were employed for calibration of High Performance Liquid Chromatography (HPLC) and Ionic Chromatography (IC). A certified gas standard mixture (CO and CO_2 balanced in N_2) purchased from Praxair was used for quantification purposes. H_2SO_4 (Panreac) and methanol were HPLC grade. Na_2CO_3 (Panreac), $NaHCO_3$ (Merck), 2,6-Pyridinedidicarboxylic acid (Sigma-Aldrich) and nitric acid (65% Panreac) were used for mobile phase preparation in IC analysis and $TiOSO_4$ (Riedel-deHaën) was employed for H_2O_2 determination. HCl (37% Panreac) was used to adjust the initial pH of the reaction media. All these reagents were of analytical grade and were used without further purification. All solutions were prepared with deionized water.

2.2. Fenton experiments

Oxidation runs were performed in a stainless steel high-pressure reactor (BR-300, BERGHOF) operated in batch mode for both gas and liquid phase. A detailed description of the set-up and the experimental procedure was described elsewhere [16]. Aqueous

solutions containing AN, 4NPH, PYR or MEA were treated by Fenton oxidation under the standard conditions of: V_L=310 mL, $C_{N\text{-}pollutant}$ = 1000 mg/L, stoichiometric dosage of H_2O_2 for complete mineralization of the selected pollutant, T= 90º C, pH_0=3, C_{Fe2+}=100 mg/L and a stirring speed of 600 rpm. After 3 h of reaction, the gas phase was collected in a Tedlar bag and analysed. Also, the liquid sample was immediately analysed. These operating conditions were selected from a previous work due to the high mineralization degree achieved in the phenol Fenton Oxidation [16].

For experiments in which CO and CO_2 were continuously monitored, the gas exit of the stainless steel high-pressure reactor (BR-300, BERGHOF) was connected to an online infrared gas analyser to monitor CO and CO_2 upon Fenton oxidation. During this reaction, 1 L/min N_2 stream was continuously flowed into the reactor to vent the reaction gas effluent, which passed through a trap of water and before entering to the detector. These oxidation experiments were carried out at lower initial concentrations of the nitrogen pollutant ($C_{N\text{-}pollutant}$ =100 mg/L) and catalyst (C_{Fe2+}=100 mg/L) to prevent signal saturation in the CO_2 detector. Other operating conditions remain unaltered (stoichiometric dosage of H_2O_2, T= 90º C and pH_0=3).

2.3. Analytical methods

Gas phase was collected in a Tedlar bag. NO_x, CO and CO_2 were measured by different techniques. NO_x species (NO + NO_2), measured both as nitrogen monoxide (NO), were quantified in a chemiluminescence CLD 60 Analyser (Ecophysics). CO_2 and CO were analysed in a GC (Bruker 3900 model) using a 30 m Carboxen 1000 column with He as carrier gas (30 mL/min). The GC was equipped with a thermal conductivity detector (TCD) set at 150 ºC, and the following temperature program was employed: 35 °C (5 min) to 200 °C at 20 °C/min, hold at 200 °C for 8 min.

For those experiments in which CO and CO_2 were on-line monitored, the gas exiting the reactor at 1 L/min (containing the Fenton off-gas and the N_2 carrier) was analysed using an Ultramat 23 infrared detector (Siemens). CO_2 and CO signals were recorded every 6 s during 15 min of reaction in ppmv. By the integration of these curves, the accumulated amounts of CO_2 and CO produced (in mg) were calculated.

AN, 4NPH and PYR were analysed by HPLC (Varian ProStar) using a C18 column (Eclipse Plus C18, 150x4.6 mm, 5 μm) at 323 K. For AN determination, elution of the mobile phase started with 80% water and 20% of methanol in volume for 1 min, then a linearly progressive gradient from 20% of methanol to 100% was executed in 3 min. For 4NPH and PYR quantification, a water/methanol mixture at 50/50 and 80/20 ratios at 1 mL/min was used as mobile phase, respectively. A photo-diode array detector at wavelengths of 230, 254 and 326 nm were used for AN, 4NPH and PYR, respectively.

MEA and NH_4^+ were analysed by IC (Metrohm 790 IC) using a Metrosep C4 column (250 x 4 mm) as stationary phase and 0.9 mL/min of a 1.7 mM aqueous HNO_3 solution with 0.775 g/L of 2,6-pyridinedidicarboxylic acid as the mobile phase. NO_3^- and NO_2^- were analysed by IC (Metrohm 883 IC) using a Metrosep A supp 5 column (250 x 4 mm) as stationary phase and 0.7 mL/min of an aqueous solution of 3.2 mM Na_2CO_3 and 1 mM $NaHCO_3$ as the mobile phase.

Total Organic Carbon (TOC) and Total Inorganic Carbon (TIC) in the liquid effluent were measured using a TOC Analyser (Shimadzu, mod. TOC-Vsch). Total Nitrogen (TN) was measured in a TOC Analyser (Shimadzu, mod. TOC-L) equipped with a TNM-L detector. Hydrogen peroxide concentration was analysed by colorimetric titration $TiOSO_4$ method in a UV2100 Shimadzu UV–vis spectrophotometer [20].

The content of on carbon, hydrogen and nitrogen of the recovered suspended solid in the AN Fenton oxidation was measured by Elemental Analysis (EA) in a LECO CHNS-932 Elementary Chemical Analyzer.

3. Results and discussion

Different experiments have been carried out using 1000 mg/L of the nitrogen-containing pollutants, the stoichiometric amount of hydrogen peroxide for its complete oxidation and 100 mg/L of Fe^{2+}. Pollutant concentration, TOC removal and H_2O_2 consumption were measured after 3 h of reaction at 90 ºC for the four-selected compounds. Data are shown in Figure 1a. The results obtained with phenol in a previous work [16] have been also included for the sake of comparison. As it can be seen, there are differences in the reactivity of these pollutants. Thereby, AN and 4NPH were completely oxidized, achieving high TOC conversions, 70 and 60%, respectively. The results obtained for AN were similar to those found for phenol at the same operating conditions. However, 4NPH oxidation rate was slower. In fact, only when the reaction was continued until total hydrogen peroxide consumption (5 h), a similar mineralization degree as with phenol was achieved (X_{TOC}=73%). On the other hand, PYR and MEA were less reactive. Only pollutant conversions of 53 and 89%, respectively, were achieved with low mineralization degrees (36 and 30%, respectively).

Attending to these results, the oxidability of the tested pollutants is: PH>AN>4NPH>>PYR>MEA. This can be explained attending to their different chemical structure. For instance, the aromatic compounds are more reactive than aliphatic. For this reason, AN was more susceptible to react with HO• species and was oxidized at a higher rate than MEA though both pollutants contain the same -NH_2 group. The low conversion of PYR (X_{PYR}=50%) comparing to the others aromatic pollutants at the same conditions (Figure 1a) can be related to the electron withdrawing effect of the

nitrogen atom, which reduces the electronic density in the ring structure [21, 22]. This effect is stronger when nitrogen is located in the ring (PYR) than when is substituent such as -NO_2 for 4NPH. In contrast, AN with an electron-donating group (-NH_2) is the most reactive nitrogen-containing pollutant.

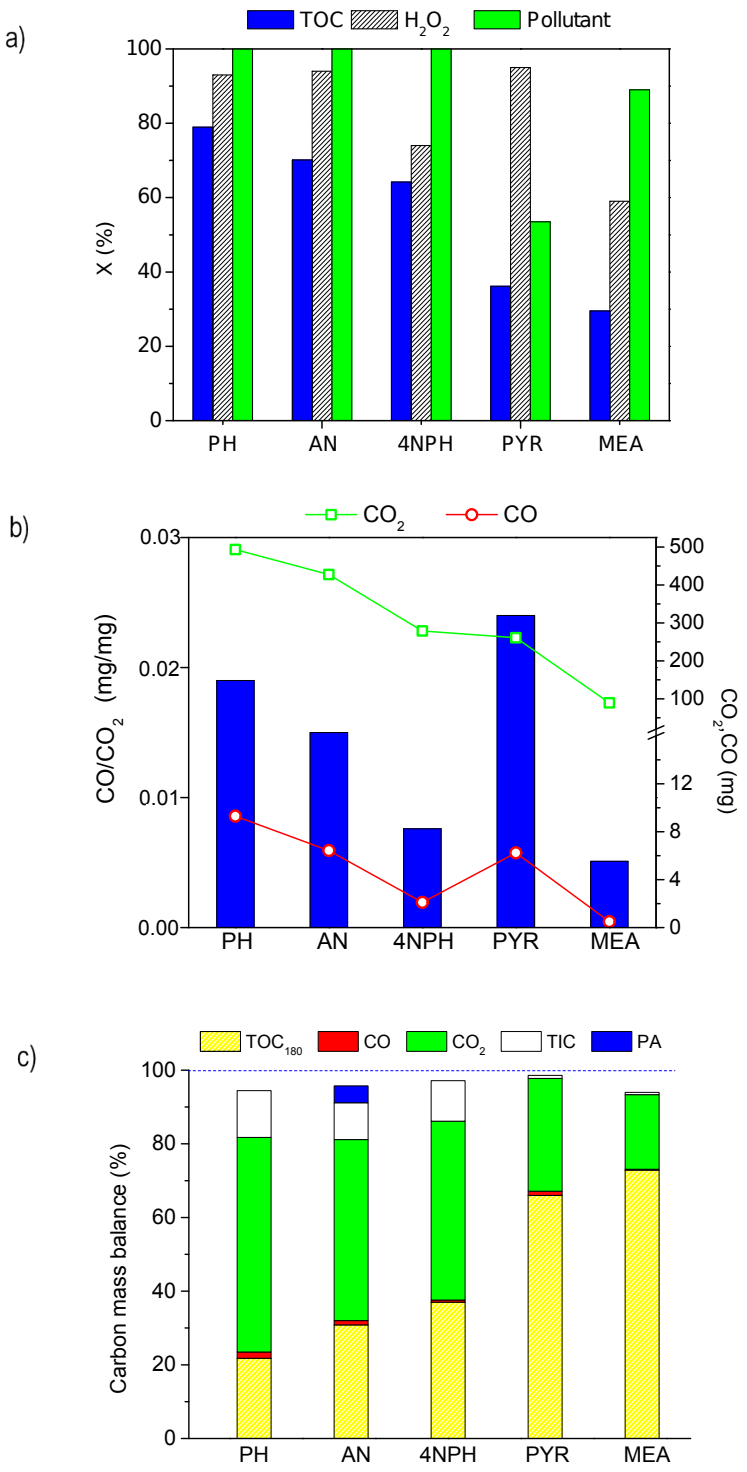

Figure 1. Results obtained in the degradation of different nitrogen-containing pollutants by Fenton oxidation at pH_0=3, $[Fe^{2+}]$=100 mg/L, T=90 °C, $[Pollutant]_0$=1000 mg/L, stoichiometric dosage of H_2O_2, and 180 min of reaction time. Pollutant, hydrogen peroxide and TOC conversions (a), CO/CO_2 ratio and total amount of CO_2 and CO (b) and carbon distribution in the off-gas (c).

3.1 CO formation and carbon mass balance

The gas phase accumulated in the reactor after 3 h of Fenton oxidation reaction was collected and analysed. The amounts of CO and CO_2 (in mg) produced along with the CO yields, represented as CO/CO_2, are provided in Figure 1b. Besides, the carbon mass balance is shown in Figure 1c, where the contribution of the gaseous products (*viz*. CO and CO_2) and the species in the liquid phase (measured as TOC and TIC) is provided in terms of carbon percentage.

As it can be observed in Figures 1a and b, the CO_2 production is in accordance to the mineralization achieved. For instance, *c.a.* 500 mg of CO_2 were quantified in the phenol Fenton oxidation at 79% of TOC removal and this value was reduced to *c.a.* 100 mg in the MEA oxidation at 30% TOC removal. Note that when the mineralization achieved is high and consequently the production of CO_2, *viz*. for PH, AN and 4NPH, the presence of CO_2 absorbed in the liquid phase (TIC) is also high. In fact, the TIC fraction represented the 10% of the total carbon (Figure 1c). Taking into account that the sum of carbon percentage in the gas and liquid phase is fairly closed to 100% for the four nitrogen-containing pollutants, see Figure 1c, the CO and CO_2 amounts measured can be considered reliable. For the mass balance of AN (Figure 1c), the solid fraction detected and measured after reaction has been also considered and was attributed to polyaniline species (PA), typically produced by AN polymerization during the oxidation process [23].

On the other hand, CO was also detected in the gas phase after 3 h of reaction for each pollutant, but this noxious species was produced in a lesser extend (from 0.5 to 9 mg, Figure 1b) than CO_2. Remarkable, the CO production seemed to depend more on the type of pollutant than on the mineralization achieved and consequently the CO yield (CO/CO_2 ratio) changed from one compound to another. In this sense, PYR notes for its high CO yield (Figure 1b). This value was unexpectedly high considering that only half of the pollutant is degraded in comparison to the total disappearance of PH, AN or 4NPH (Figure 1a). These results point out that the ring opening of the PYR must occur in such a way as to favour the CO production.

In the AN oxidation, a dark suspended solid was formed once the H_2O_2 was injected. After 3 h of reaction, the solid was recovered by evaporation of the liquid effluent, weighted and analysed by EA. It had the non-negligible contribution of *c.a.* 5% to the carbon mass balance and a composition similar to polyaniline species (see Table S1 of the Supplementary Material). Precisely, the significant presence of these condensation products can be the reason for the slightly lower CO yield for AN compared to PH.

As can be observed in Figure 1b, significant low CO/CO_2 ratios were found for 4NPH compared to PH. This can be explained by the fact that 4NPH is favourably oxidised through catechol route instead of hydroquinone [24], being the former less selective to CO, as it has been reported in a previous work [16].

In the case of MEA, a minor CO production was detected (0.5 mg) and the CO/CO_2 ratio was negligible, which is accordance to the aliphatic nature of this compound [16].

In order to gain an insight into the emission of gaseous species upon Fenton oxidation and in particular on the CO yield of the different nitrogen containing pollutants, the continuous monitoring of the gas effluent was carried out to analyse the evolution of CO

and CO_2 during 15 min of reaction (at 90 ºC and 100 mg/L of pollutant). The data recorded in the analyser as ppmv of CO and CO_2 released in the exit gas are given in Figures 2a and b. As it can be seen, there is a significant peak of CO and CO_2 at the beginning of the reaction, from 1 to 2 min, for the most oxidable compounds, *viz.* PH, AN and 4NPH, and eventually decreases with the reaction time. This observation indicates that the mineralization occurs immediately after the injection of H_2O_2. For PH, the most reactive pollutant, the peaks are observed at 1 min of the reaction and the signal of CO and CO_2 (in ppmv) are significantly higher than for AN (*c.a.* 1.5 min) and 4NPH (*c.a.* 2 min.). Interestingly, PYR shows an increase of the CO signal at 1 min reaction time while the CO_2 detected was very low, results consistent with its highest CO yield (Figure 1b). Also, as expected according to the previous results (Figure 1) and the lower pollutant concentration employed in these experiments (100 ppm), the CO signal monitored upon MEA oxidation were negligible, being at the threshold of the detection of the equipment.

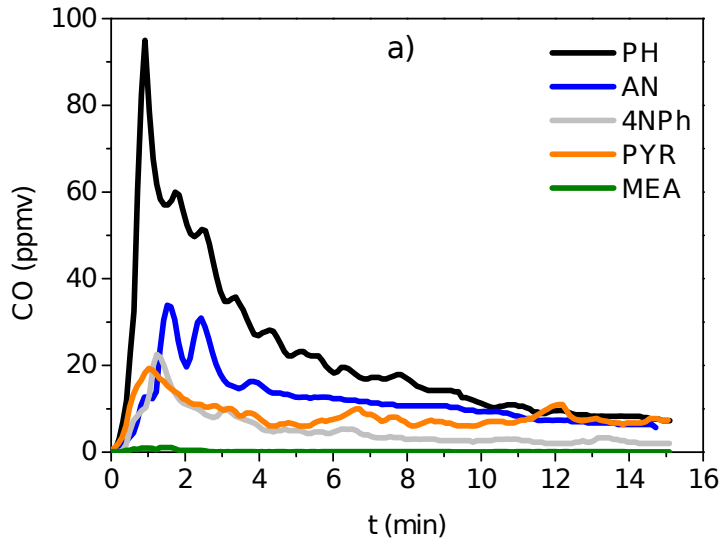

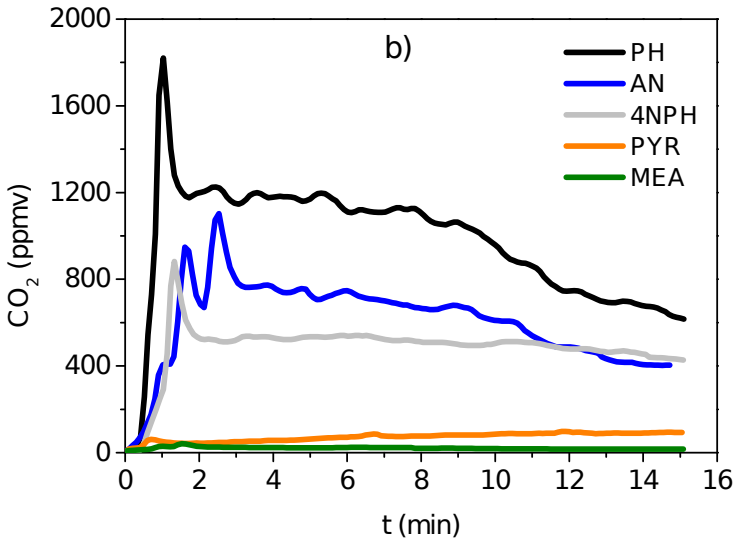

Figure 2. CO (a) ad CO_2 (b) released in the gas effluent obtained in the degradation of different nitrogen-containing pollutants by Fenton oxidation at the following operating conditions: $[Pollutant]_0$=100 mg/L, stoichiometric dosage of H_2O_2, $[Fe^{2+}]$=100 mg/L, T=90 °C and 15 min reaction time.

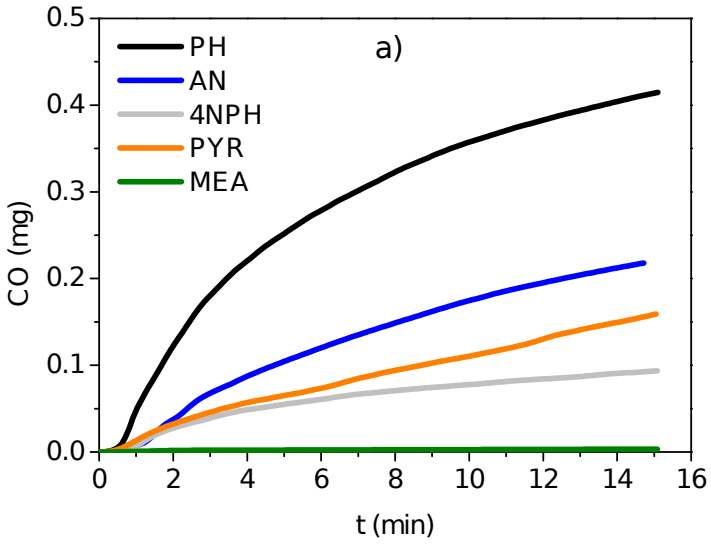

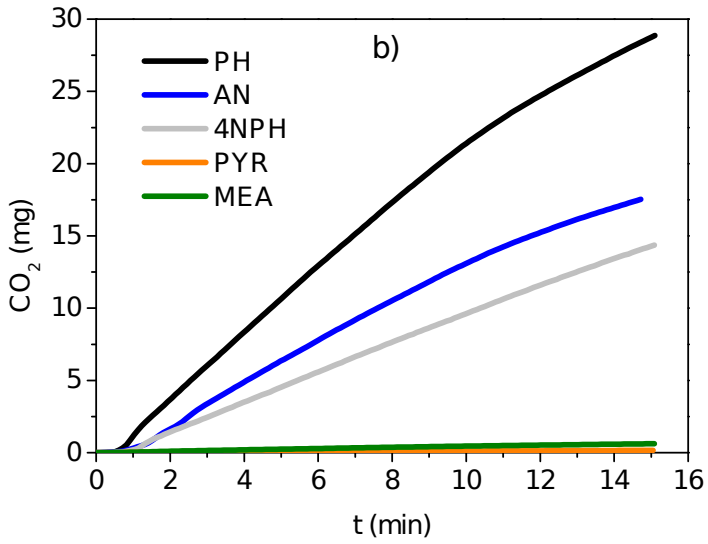

Figure 3. Temporal profiles of the accumulated amount of CO (a) and CO_2 (b) obtained in the degradation of different nitrogen-containing pollutants by Fenton oxidation at the following operating conditions: $[Pollutant]_0$=100 mg/L, stoichiometric dosage of H_2O_2, $[Fe^{2+}]$=100 mg/L, T=90 °C and 15 min reaction time.

Figure 3 provides the accumulated amounts of CO and CO_2 (in mg) calculated from the data recorded in Figure 2. It is remarkable that for PH, AN and 4NHP, CO is faster produced at the beginning of the reaction and tends towards an asymptotic value within the 15 min of the experiment (Figure 3a). In contrast, the CO_2 release seems to be continued upon reaction time (Figure 3b). These observations are consistent with the fact that CO is mainly formed during the oxidative cleavage of aromatic rings [16], which are the first intermediate species analysed in the reaction media. As long as they are oxidized and the initial compound is removed (see Figure S2 of the Supplementary Material), the CO production becomes negligible. However, CO_2 is progressively formed through the mineralization of the remaining different intermediates. On the contrary, in the case of PYR, the CO asymptotic value is not observed within the 15 min because the PYR conversion is low (see Figure S2) and consequently the aromatic intermediates are expected to be present in the media. Due to the low amounts of CO detected for MEA,

conclusive results regarding the CO yields cannot be drawn, nevertheless these results points out that CO production is minimized when this type of aliphatic pollutants are oxidised.

Finally, the evolution of the CO/CO_2 ratio represented in Figure 4 shows the prominent values for PYR, for which a high CO/CO_2 ratio is maintained upon the reaction time, due to the low progress of the oxidation reaction upon the 15 min time of the monitoring (Figure S2). Also high CO yields can be observed for PH and 4NPH at the beginning of the reaction which is indicative of the ring cleavage of the aromatic species. For AN, this behaviour is more moderate probably because initially the aniline also condensates to polyanilines.

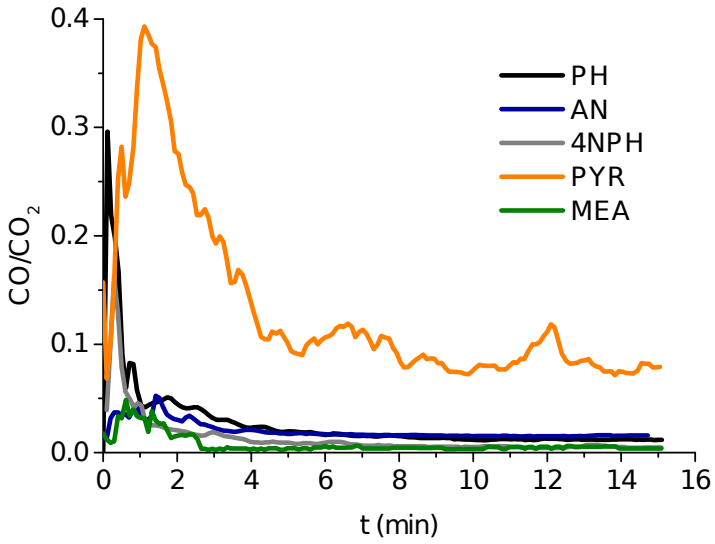

Figure 4. Evolution of CO yields, expressed as CO/CO_2 ratio (in mg), during the degradation of different nitrogen-containing pollutants by Fenton oxidation at the operating conditions of Figure 2.

3.2. Nitrogen by-products and mass balance

The concentration of nitrogen oxides such as NO and NO_2, lumped as NO_x species, were measured in the gas phase after 3 h of oxidation carried out at 1000 ppm of initial pollutant

and 90 ºC. The results obtained for each pollutant are provided in Figure 5a. As it can be observed, NO_x was produced in trace amounts (< 1 mg/Nm^3) for AN, 4NPH and PYR, while for aliphatic compounds such as MEA, NO_x was not produced or at such low levels that it could not be measured. As it can be discerned from Figure 5a, those pollutants with -NO_2 groups, as 4NPH, favours the production of NO_x. These results are in accordance to those semi-quantitatively estimated by García-Segura et al. [17] during the electrooxidation of nitro and amino benzoic acids.

Though the contribution of nitrogen as NO_x species was negligible to the nitrogen mass balance, the levels of NO_x released upon Fenton processes should not be underestimated as demonstrated by the fact that the concentration of NO_x upon the 4NPH oxidation at 3 h of reaction (*c.a.* 1 mg/Nm^3) exceeded the limit values of NO_2 in air (40 μg/m^3) for the protection of human health according to the Directive 2008/50/EC [25].

The distribution of the nitrogen containing by-products in the liquid phase after 3 h of reaction is given in Figure 5b. The inorganic nitrogen species measured were ammonia (NH_4^+), nitrite (NO_2^-) and nitrate (NO_3^-). The rest of nitrogen required to achieve the TN_{180} value (total nitrogen in the liquid effluent after 3 h of reaction) was attributable to the remaining initial pollutant and undetermined nitrogen by-products such as formamides or acetamides, very common in MEA oxidation [26,27].

The nature of the nitrogen functional group in the organic pollutant affects the distribution of N-species by-products (Figure 5b). Thus, AN and MEA, with an amino group, mainly yielded NH_4^+. 4NPH, with a nitro group, gave rise to NO_3^- while NH_4^+ was formed in very low concentration. In the case of a pyridine, the predominant species was NH_4^+, though NO_3^- and NO_2^- were also detected in low amounts.

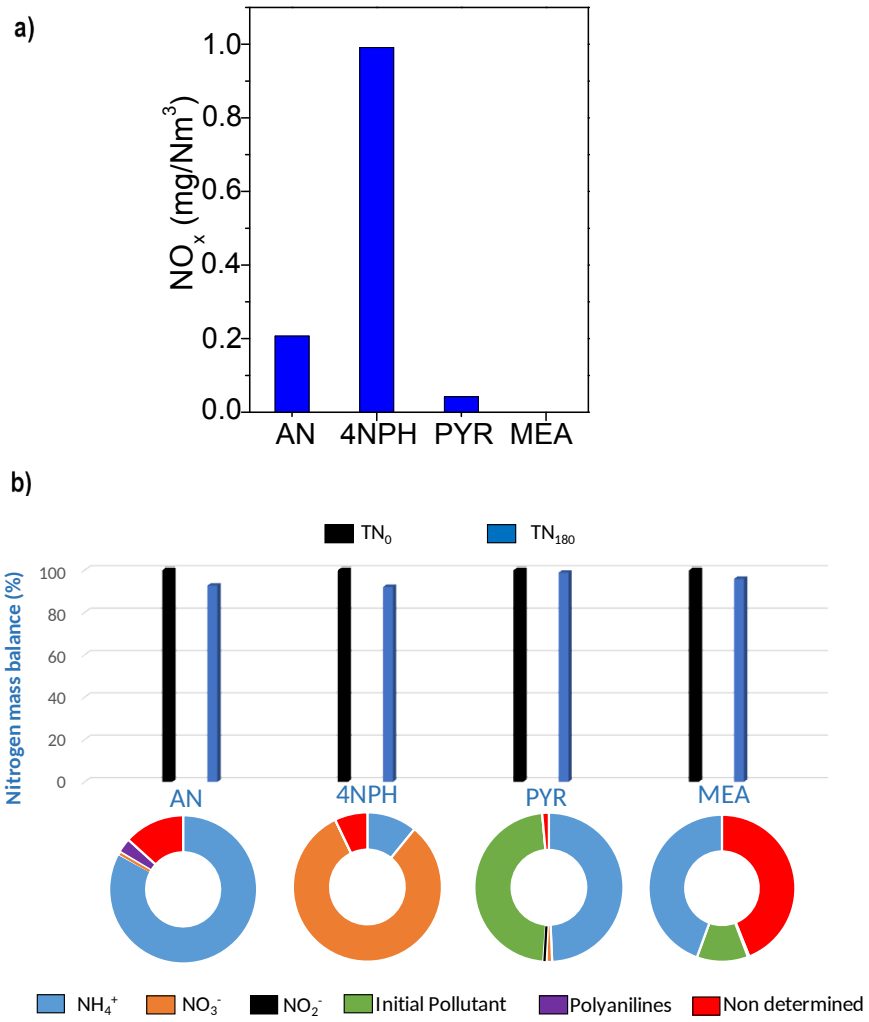

Figure 5. Concentration of NO_x in the off-gas (b) and nitrogen distribution in the liquid effluent (b) after 180 min reaction on the Fenton oxidation of the selected pollutants at the operating conditions of Figure 1.

Finally, as can be observed in Figure 5b, the differences between the initial (TN_0) and final (TN_{180}) total nitrogen in the liquid phase varied from 1.1 % for PYR to 7.5% for AN. These differences revealed a decrease of nitrogen mass in the liquid phase during the oxidation process that cannot be explained by the low amounts of NO_x detected in this work. Thus, other possible nitrogen by-products such as solid condensation products containing nitrogen or gaseous species as N_2 cannot be discarded [17,18,23].

4. Conclusions

The results of this work highlight the importance of monitoring the gas phase generated during the treatment of high-loaded wastewater containing nitrogen organic pollutants by Fenton Oxidation Process in order to guarantee the environmental sustainability of the process, and also to properly follow the progress of the reaction.

The nature of the organic compound (aromatic or aliphatic), the nitrogen functional group (viz. $-NH_2$, $-NO_2$), or the presence of N in a heterocyclic compound (pyridine) determine the oxidability of the pollutants and have repercussion on the emission of gaseous species.

The main conclusions achieved are:

- CO_2 is the main gaseous compound and it is progressively formed upon Fenton oxidation
- The CO production ($\sim 10^4$ mg/Nm^3) is simultaneous to the rupture and opening of the aromatic ring.
- CO yields are significantly higher when the nitrogen is part of the aromatic ring, as in the case of pyridine.
- NO_x production is favoured in presence of $-NO_2$ group ($\sim$1 mg/Nm^3) but its contribution to nitrogen mass balance is negligible.
- N-species by-products mainly remain in the liquid phase: amino group and pyridine majorly yields NH_4^+, and nitro group to NO_3^-.

Acknowledgments

Financial support from the project CTM2016-76454-R (Ministerio de Economía y Competitividad-MINECO, Spain) is gratefully acknowledged.

References

[1] A.R. Ribeiro, O.C. Nunes, M.F.R. Pereira, A.M.T. Silva. An overview on the advanced oxidation processes applied for the treatment of water pollutants defined in the recently launched Directive 2013/39/EU. Environ. Inter. 75 (2015) 33–51.

[2] M. A. Oturan, J. J. Aaron, Advanced oxidation processes in water/wastewater treatment: Principles and applications. Crit. Rev. Env. Sci. Tec. 44 (2014) 2577-2641.

[3] D. B. Miklos, C. Remy, M. Jekel, K. G. Linden, J. E. Drewes, U. Hübner, Evaluation of advanced oxidation processes for water and wastewater treatment - A critical review. Water Res. 139 (2018) 118-131

[4] D. Mantzavinos, E. Psillakis, Enhancement of biodegradability of industrial wastewaters by chemical oxidation pretreatment J. Chem. Technol. Biotechnol. 79:431–454 (online: 2004).

[5] K.E. Campos Díaz, J.L. Álvarez Cruz, M.L. Rodríguez, E.R. Bandala, Coupled Inverse Fluidized Bed Bioreactor with Advanced Oxidation Processes for Treatment of Vinasse AIMS Geosciences, 3 (2017) 538-551.

[6] M. Cheng, Yang Liu, D. Huang, C. Lai., G. Zeng, J. Huang,, Z. Liu, C. Zhang, C. Zhou, L. Qin, W. Xiong, H. Yi, Y. Yang. Prussian blue analogue derived magnetic Cu-Fe oxide as a recyclable photoFenton catalyst for the efficient removal of sulfamethazine at near neutral pH values, Chem. Eng. J. 362 (2019) 865-876

[7] Y. Chen, J. Lin, Z. Chen, Remediation of water contaminated with diesel oil using a coupled process: Biological degradation followed by heterogeneous Fenton-like oxidation. Chemosphere, 183 (2017) 286-293.

[8] Industrial Emissions Directive 2010/75/EU Best Available Techniques (BAT) Reference Document for Common Waste water and Waste Gas Treatment/Management

Systems in the Chemical Sector http://eippcb.jrc.ec.europa.eu/reference/BREF/CWW_Final_Draft_07_2014.pdf

[9] C. Comninellis, A. Kapalka, S. Malato, S.A Parsons, I. Poulios and D. Mantzavinos. Advanced oxidation processes for water treatment: advances and trends for R&D, J. Chem. Technol. Biotechnol. 83 (2008) 769–776.

[10] N. Wang, P. Wang, Study and application status of microwave in organic wastewater treatment – A review. Chem. Eng. J. 283 (2016) 193–214.

[11] R. Dewil, D. Mantzavinos, I. Poulios, M. A. Rodrigo, New perspectives for Advanced Oxidation Processes. J. Environ. Manage. 195 (2017) 93-99

[12] G. Boczkaj, A. Fernandes, Wastewater treatment by means of advanced oxidation processes at basic pH conditions: A review. Chem. Eng. J. 320 (2017) 608–633.

[13] P. Qiu , B. Park, J. Choi, A. B. Pandit, J. Khim. A review on heterogeneous sonocatalyst for treatment of organic pollutants in aqueous phase based on catalytic mechanism. Ultrason. Sonochem. 45 (2018) 29-49.

[14] V. Poza-Nogueiras, E. Rosales, M. Pazos, M. A. Sanromán. Current advances and trends in electro-Fenton process using heterogeneous catalysts – A review. Chemosphere, 201 (2018) 399-416.

[15] M. Sillanpää, M.C. Ncibi, A. Matilainen, Advanced oxidation processes for the removal of natural organic matter from drinking water sources: A comprehensive review. J. Environ. Manage. 208 (2018) 56–76.

[16] J. Carbajo, A. Quintanilla, J. A. Casas, Assessment of carbon monoxide formation in Fenton process: the critical role of pollutant nature and operating conditions, Appl. Catal. B Environ. 232 (2018) 55–59.

[17] S. Garcia-Segura, E. Mostafa, H. Baltruschat, Could NOx be released during mineralization of pollutants containing nitrogen by hydroxyl radical? Ascertaining the release of N-volatile species. Appl. Catal. B: Environ. 207 (2017) 376–384.

[18] C. Lousteau, M. Besson, C. Descorme, Catalytic wet air oxidation of ammonia over supported noble metals. Catal. Today 241 (2015) 80–85.

[19] P. Bautista, A.F. Mohedano, J.A. Casas, J.A. Zazo, J.J. Rodriguez, An overview of the application of Fenton oxidation to industrial wastewaters treatment. J. Chem. Technol. Biotechnol. 83 (2008) 1323–1338.

[20] G. Eisenberg, Colorimetric determination of hydrogen peroxide, Ind. Eng. Chem. Anal. Ed. 15 (1943) 327–328.

[21] A. G. Agrios, P. Pichat, Recombination rate of photogenerated charges versus surface area: opposing effects of TiO2 sintering temperature on photocatalytic removal of phenol, anisole, and pyridine in water. J. Photochem. Photobiol. A Chem. 180 (2006) 130-135.

[22] Y. Li, R. Yi, C. Yi, B. Zhou, H. Wang, Research on the degradation mechanism of pyridine in drinking water by dielectric barrier discharge. J. Environ. Sci. 53 (2017) 238-247.

[23] A. Benito, A. Penades, J. L. Lliberia, R. Gonzalez-Olmos, Degradation pathways of aniline in aqueous solutions during electrooxidation with BDD electrodes and UV/H_2O_2 treatment. Chemosphere 166 (2017) 230-237

[24] V. Kavitha, K. Palanivelu, Degradation of nitrophenols by Fenton and photo-Fenton processes. J. Photochem. Photobiol. A Chem. 170 (2005) 83-95

[25] Directive 2008/50/EC of the European Parliament and of the Council of 21 May 2008 on ambient air quality and cleaner air for Europe. Off. J. Eur. Union, 152 (2008), pp. 1-44

[26] E. F. da Silva, H. Lepaumier, A. Grimstvedt, S. J. Vevelstad, A. Einbu, K. Vernstad, H. F. Svendsen, K. Zahlsen, Understanding 2-Ethanolamine Degradation in Postcombustion CO_2 Capture. Ind. Eng. Chem. Res. 51 (2012) 13329-13338

[27] C. Gouedard, D. Picq, F. Launay, P.-L. Carrette, Amine degradation in CO_2 capture. I. A review. Int. J. Greenh. Gas. Con. 10 (2012) 244-270

Characterization of the gas effluent in the treatment of nitrogen containing pollutants by Fenton Process

J. Carbajo*, A. Quintanilla, J.A. Casas

Chemical Engineering Department, Universidad Autonoma de Madrid, Ctra. Colmenar km. 15, 28049 Madrid, Spain.

*Corresponding author: jaime.carbajo@uam.es

Supplementary Material

Table S1. The relative content of carbon, hydrogen and nitrogen (wt.%) in the suspended solid recovered after 3 h of AN Fenton oxidation. Measured by Elemental Analysis in a LECO CHNS-932 Elementary Chemical Analyzer. Comparison to the theoretical content in polyaniline (leucoemeraldine base $[C_6H_4NH]_n$)

	C	**H**	**N**
Suspended solid	83.5	6.6	9.9
Theoretical polyamine	86.8	3.5	9.7

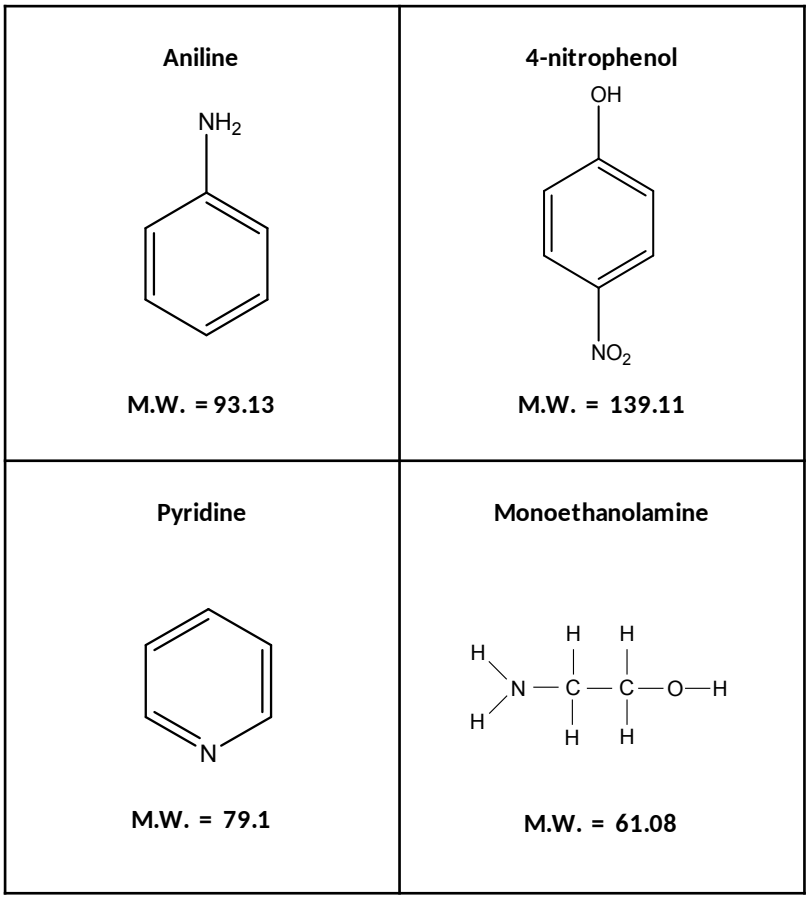

Figure S1. Chemical structure of the nitrogen containing pollutants.

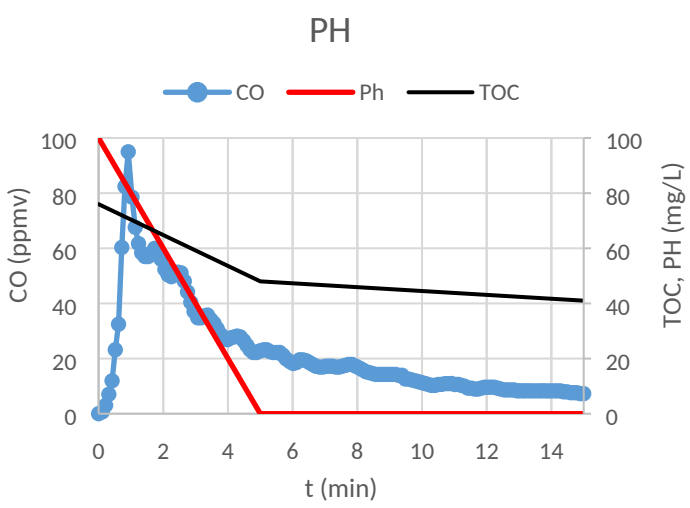
PH
CO
Ph
TOC
CO (ppmv)
TOC, PH (mg/L)
t (min)

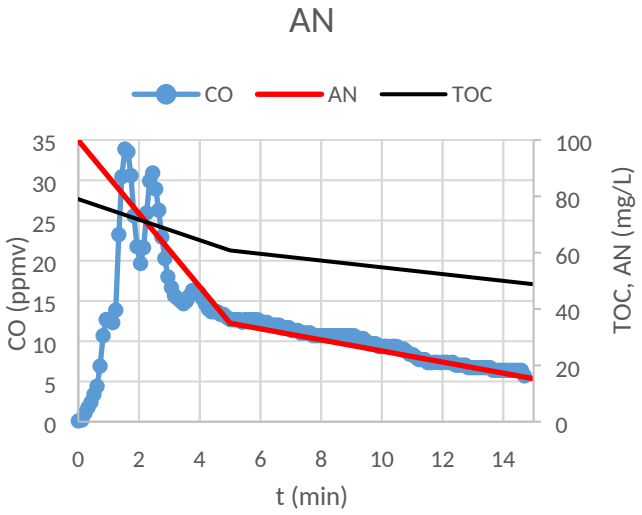
AN
CO
AN
TOC
CO (ppmv)
TOC, AN (mg/L)
t (min)

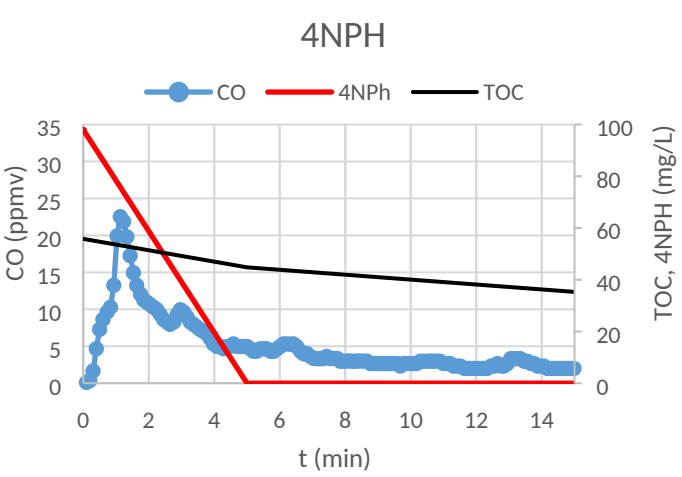
4NPH
CO
4NPh
TOC
CO (ppmv)
TOC, 4NPH (mg/L)
t (min)

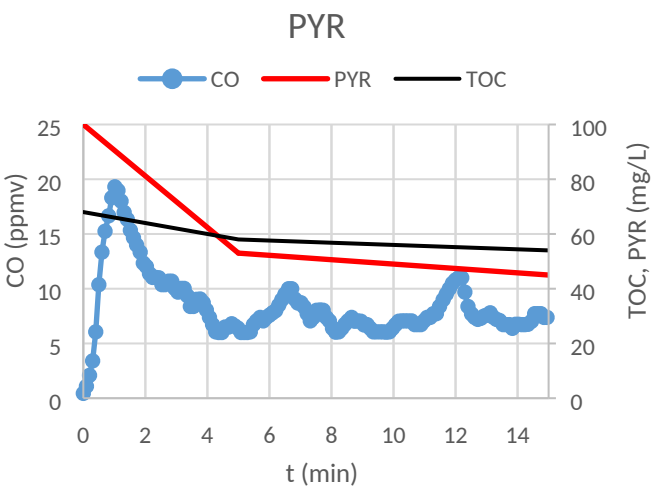
PYR
CO
PYR
TOC
CO (ppmv)
TOC, PYR (mg/L)
t (min)

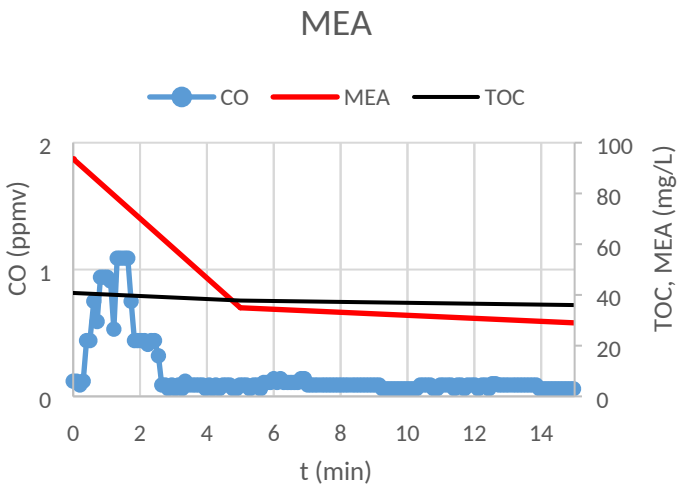
MEA
CO
MEA
TOC
CO (ppmv)
TOC, MEA (mg/L)
t (min)

Figure S2. Temporal profiles of pollutant, TOC and CO concentrations upon Fenton oxidation at the following operating conditions: $[Pollutant]_0$=100 mg/L, stoichiometric dosage of H_2O_2, $[Fe^{2+}]$=10 mg/L, T=90 °C.